# Shape fluctuations of crystal bars

D. E. Wolf and J. Villain*
*Institut für Festkörperforschung, Kernforschungsanlage Jülich G.m.b.H., D-5170 Jülich, Federal Republic of Germany*
(Received 26 May 1989)

In the standard theory of the equilibrium shape of a crystal (Wulff construction), thermal fluctuations are neglected. In the present work their effect is investigated in the simple case of a bar with four symmetric facets. The edges of the facets are found to undergo fluctuations with a correlation length proportional to the width $2R$ of the facets, which is itself proportional to the diameter of the bar. The amplitude of these fluctuations decays exponentially beyond a range proportional to $R^{1/3}$. It is therefore legitimate to neglect them for large crystals. The stability of the bar is also considered: The decay into crystallites is very slow with a characteristic time increasing exponentially with $R$.

## I. INTRODUCTION

In recent years a number of new results have been derived concerning the equilibrium shape of crystals, one of the most prominent and well-understood capillary effects (for a review see, e.g., Refs. 1 and 2). Among these results, the way in which the rounded part of a surface joins a facet deserves special attention. For vicinal orientations (close to that of the facet), one may view the surface as consisting of steps separated by terraces. Based on investigations of the interaction between these steps (either elastically or by steric repulsion), it has been predicted that the curvature of the rounded part diverges at the facet edge.[3] This singular behavior is only obtained in the limit of large samples. Therefore its experimental confirmation is difficult[4], and its validity is still debated.[5]

Here we present a calculation of fluctuation corrections to the equilibrium shape. Their magnitude will be found to be negligible for large samples: They are, in this sense, a finite-size effect. Although our results cannot directly be compared with experiments, they may point into a direction in which a solution can be found for the discrepancies between theoretical predictions and measurements on finite samples.

We consider a container of fixed volume $V$ with a fixed total mass $M$ chosen such that the system separates into a crystal of volume $V_c$ surrounded by the vapor or melt of the same material. (It is well known that one has to consider a canonical ensemble in order to have stable coexistence of two phases. If the system were allowed to exchange particles with a particle reservoir, it would always prefer to be in a single phase, thereby removing all interface contributions to the grand potential.) We adopt the Gibbs convention, i.e., $V_c$ and the volume of the fluid, $V_f$, are determined by

$$V=V_c+V_f$$

and (1.1)

$$M=M_c+M_f=\rho_c V_c+\rho_f V_f$$

with the mass densities $\rho_c$ and $\rho_f$. Let

$$\hat{F}=F_c+F_f+F_s \tag{1.2}$$

be the free energy (including the surface excess part $F_s$) calculated for a particular surface configuration. Performing the trace over all surface configurations (not just minimizing $\hat{F}$ as in the Wulff construction) leads to the equilibrium free energy

$$F(T,V,M)=-k_B T\ln Z,\quad Z=\mathrm{Tr}\exp(-\beta\hat{F})\ . \tag{1.3}$$

Equation (1.3) contains the thermal fluctuations of the equilibrium shape that we want to calculate.

We use the following model to describe the surface configurations and their free energy. The crystal forms an infinite bar (Fig. 1) with four equivalent facets parallel to the $xy$ and $zy$ planes, respectively. By symmetry we can restrict ourselves to one-eighth of the bar (hatched part in Fig. 1). We shall regard the curved part as consisting of $p$ ledges of atomic height separated by terraces (Fig. 2). No upward ledges are taken into account so that in particular no islands on the terraces occur in our model. It will be assumed that no overhangs are present so that the position of the $m$th ledge at a given ordinate $y$ is a well-defined number $x_m(y)$ and satisfies

$$x_{m-1}(y)\le x_m(y)\le x_{m+1}(y)\ . \tag{1.4}$$

Thermal vibrations and elastic strains will be ignored [solid-on-solid (SOS) model]. Therefore, $x_m(y)$ can only be changed by adding or removing atoms, i.e., it is an integer.

To regard the crystal as incompressible turns out to be a useful simplification also in view (1.1): $\rho_c$ is a constant independent of $V_c$, while $\rho_f(V,M,V_c)$ is determined by (1.1):

$$\rho_f=(M-\rho_c V_c)/(V-V_c)\ . \tag{1.5}$$

At finite temperatures the ledges will not be straight lines. They will have kinks, each with an excitation ener-

 

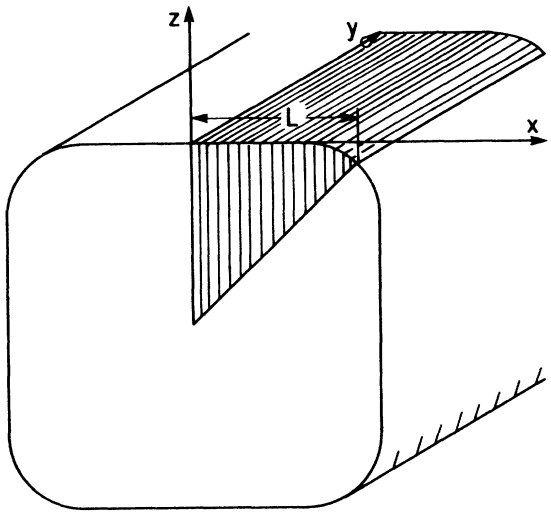


FIG. 1. A crystalline bar with four facets parallel to the $xy$ and $zy$ planes extending to infinity along the $y$ direction.

gy $\tau_1$. We shall assume that the temperature is low enough, $\beta\tau_1 \gg 1$, so that the kinks form a very dilute one-dimensional gas on a ledge and their interactions can be ignored.

A short-range, repulsive interaction between the ledges will be assumed; for instance,

$$U=\sum_{m=1}^{p}\sum_{y=1}^{N} v(x_{m+1}(y)-x_m(y)) , \tag{1.6}$$

where $N$ is the length of the bar measured in lattice constants. An attractive or oscillating interaction would favor other facets,[6] which we do not want to consider here. Equation (1.4) implies

$$v(x)=\infty \quad \text{for } x<0 . \tag{1.7}$$

Denoting the surface tension of the facet and of the terraces between the ledges by $\alpha$, and the energy per unit length of the straight parts of a ledge by $\tau_0$, the surface free energy of $\frac{1}{8}$ of the bar is given by

$$F_s/8=\alpha LN+\tau_0 pN+\tau_1\sum_{m,y}|x_m(y+1)-x_m(y)|+U . \tag{1.8}$$

Of course, outside the vicinal region where the width of the terraces is no longer large compared to atomic distances, one has to expect that $\alpha$ changes. However, we can imagine these corrections to be absorbed in $U$, (1.6). Similar remarks can be made for the second term in (1.8). This model is admittedly oversimplified. It is believed to capture the essence of the fluctuations in the vicinal region where the curved part smoothly joins the facet—the main focus of this paper. However, it has to be regarded with some caution near $m=p$.

To complete the definition of the model we have to discuss the bulk contribution $F_b=F_c+F_f$ to the free energy (1.2) which depends on the surface configuration through

$$V_c/8=\tfrac{1}{2}L^2N+\sum_{m,y}x_m(y) \tag{1.9}$$

(Fig. 2). We can avoid specifying the equations of state by assuming we already knew the equilibrium value $V_c^{\rm eq}(T,V,M)$ of the crystal volume, and expanding $F_b$ around it:

$$F_b=F_b^{\rm eq}-\lambda(V_c-V_c^{\rm eq})+\tfrac{1}{2}K(V_c-V_c^{\rm eq})^2/(V-V_c^{\rm eq}) . \tag{1.10}$$

Regarding $V_c^{\rm eq}$ as a fixed parameter we may use (1.10) to calculate the equilibrium surface configuration and hence the thermal expectation value $\langle V_c\rangle$. It depends on $V_c^{\rm eq}$ and has to be determined self-consistently in the end such that

$$\langle V_c\rangle(V_c^{\rm eq})=V_c^{\rm eq} . \tag{1.11}$$

The coefficients $\lambda$ and $K$ in (1.10) are given by

$$\lambda=-f_c+f_f+\mu_f(\rho_c-\rho_f^{\rm eq}) \tag{1.12}$$

and

$$K=[\kappa_f\rho_f^{\rm eq2}]^{-1}(\rho_c-\rho_f^{\rm eq})^2 . \tag{1.13}$$

The free-energy density $f_f(T,\rho_f^{\rm eq})$, the chemical potential $\mu_f(T,\rho_f^{\rm eq})$, and the isothermal compressibility $\kappa_f(T,\rho_f^{\rm eq})$ of the fluid around the crystal bar are determined by the equilibrium fluid density (1.5) for $V_c=V_c^{\rm eq}$. Using standard thermodynamic relations $\lambda$ can be related to the supersaturation in the fluid,[7] as a measure of which we take the deviation $\Delta\mu_f=\mu_f(T,\rho_f^{\rm eq})-\mu_0(T)$ of the chemical potential from its bulk coexistence value $\mu_0$. It is well known from the Laplace-Kelvin laws that $\Delta\mu_f$ becomes arbitrarily small for large diameters of the bar. Expanding $\lambda$ to lowest order in $\Delta\mu_f$ one obtains[7]

$$\lambda\sim\Delta\mu_f(\rho_c-\rho_{f0}) , \tag{1.14}$$

where $\rho_{f0}$ is the fluid density at bulk coexistence.

Equations (1.8)–(1.10) specify the model to be investi-

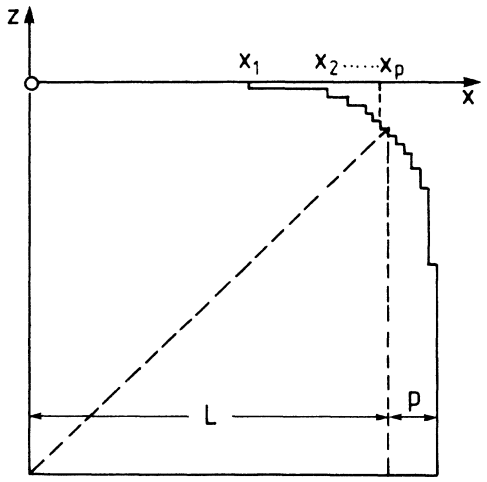


FIG. 2. The rounded surface part between two facets is represented by steps of atomic height separated by terraces.

gated in the subsequent sections. Since we are mainly interested in the ledge fluctuations close to the facet, we shall determine the equilibrium values of $L$ and $p$ (assumed to be constant along the bar) simply by minimizing the free energy. Using (1.10), this requires

$$0=\frac{\partial}{\partial L}(F_s-\lambda V_c)|_{\rm eq} \tag{1.15}$$

and

$$0=\frac{\partial}{\partial p}(F_s-\lambda V_c)|_{\rm eq} . \tag{1.16}$$

The trace in (1.3) will only be taken over all ledge configurations for fixed $L$ and $p$. Then the crystal volume cannot fluctuate by a larger amount than $8pL$. This may always be assumed to be much smaller than the volume occupied by the fluid:

$$|V_c-V_c^{\rm eq}|<8pL\ll V-V_c^{\rm eq} . \tag{1.17}$$

Therefore, the last term in (1.10) may be neglected as far as the ledge configurations are concerned. For our purpose it thus suffices to consider

$$\Omega\equiv(F_s-\lambda V_c)/8 . \tag{1.18}$$

It is instructive to separate the part $\mathcal{H}$ of $\Omega$ that governs the ledge fluctuations:

$$\Omega=N[\alpha L+\tau_0 p-(\lambda/2)L^2]+\mathcal{H} , \tag{1.19}$$

where

$$\mathcal{H}=\sum_{m,y}[\tau_1|x_m(y+1)-x_m(y)| +v(x_{m+1}(y)-x_m(y))-\lambda x_m(y)] . \tag{1.20}$$

Without the last term, $\mathcal{H}$ would be translationally invariant. Therefore, it would result in a homogeneous distribution of the $p$ steps over the interval $L$, i.e., a flat surface. The supersaturation $\lambda$ of the fluid surrounding the bar acts like an external force on the ledges that pulls them to the right (corresponding to crystal growth) (Fig. 2). In equilibrium this external force is counterbalanced by the interaction between the ledges.[8] The result is the curved equilibrium shape. The last term in (1.20) can thus be viewed as an external potential energy of the ledges.

In Sec. II it will be recalled how the surface profile is determined from (1.19) neglecting fluctuations.[9] Then, in Sec. III, a transfer-matrix calculation of the thermal fluctuations of the ledges on the curved surface will be presented. The physical implications are described in Sec. IV.

In the long run the bar geometry will not be stable. The decay into crystallites begins with small variations of $L$ along the bar. In Sec. V it will be shown, that the time scale involved in this instability is extremely long, justifying the picture put forward in the earlier parts of the paper. Section VI contains a summary of our results as well as a discussion of the influence of gravity[10] and of other possible extensions of our calculation.

## II. PROFILE WITHOUT FLUCTUATIONS

In this section the theory of Schulz[6] is briefly recalled (or, perhaps, reinterpreted). A similar account has recently been published by Parshin *et al.*[9] The shape of the bar is determined assuming that the $y$ coordinate can be integrated out in (1.20), and that the resulting free energy has the form (for $\frac{1}{8}$ of the bar)

$$\Omega=N\left[\sum_{m=1}^{p}[f(\bar{x}_{m+1}-\bar{x}_m)-\lambda\bar{x}_m] +\alpha L+\tau p-(\lambda/2)L^2\right] . \tag{2.1}$$

Here, $\bar{x}_m$ is the average value of $x_m(y)$, and

$$\bar{x}_{p+1}=L . \tag{2.2}$$

The assumption that $f$ depends only on the average distance between *nearest-neighbor* ledges is crucial because, then, $f$ can be calculated for infinite, planar surfaces with fixed orientations. Theories of Gruber and Mullins,[11] Pokrovskii and Talapov[12] or Villain[13] yield for large $l$

$$f(l)\approx\frac{\pi^2}{3}\frac{G}{l^2} , \tag{2.3}$$

and for the step free energy per unit length

$$\tau=\tau_0-2G , \tag{2.4}$$

where $G$ goes to zero at low temperatures as

$$G=k_BT\exp(-\beta\tau_1) . \tag{2.5}$$

The expressions (2.3) and (2.4) are not applicable outside the vicinal regime. More generally, in this section we shall regard $f(l)$ as a phenomenological function with asymptotic behavior (2.3). For the moment we need not specify $f(l)$ any further. At the end of this section we shall briefly discuss the additional constraint $f(l)$ has to fulfill so that the crystal does not form a sharp edge at $x=L$.

The equilibrium shape for given supersaturation $\lambda$ is determined by minimizing $\Omega$ with respect to $\bar{x}_m$ $(m=1,\ldots,p)$:

$$\begin{aligned} &f'(\bar{x}_2-\bar{x}_1)=-\lambda , \\ &f'(\bar{x}_{m+1}-\bar{x}_m)=f'(\bar{x}_m-\bar{x}_{m-1})-\lambda, \quad 2\le m\le p . \end{aligned} \tag{2.6}$$

The result of this recursion is

$$f'(l_m)=-\lambda m , \tag{2.7}$$

where $l_m$ denotes the width of the $m$th terrace,

$$l_m=\bar{x}_{m+1}-\bar{x}_m . \tag{2.8}$$

Combining (2.7) with (2.3) yields the well-known power-law shape

$$\bar{x}_{m+1}-R=\sum_{n=1}^{m}\left[\frac{3c}{2\pi^2}n\right]^{-1/3}\approx\frac{1}{c}\left[\frac{3\pi}{2}cm\right]^{2/3} \tag{2.9}$$

close to the facet. $R=\bar{x}_1$ is half the diameter of the facet, and

$$c=\lambda/G \ , \tag{2.10}$$

the dimensionless supersaturation. As $m$ is the negative $z$ coordinate of the terrace between $\bar{x}_m$ and $\bar{x}_{m+1}$, we can also write

$$cz(x)=\begin{cases}(-2/3\pi)[c(x-R)]^{3/2}, & x>R\\ 0, & x\le R \ .\end{cases} \tag{2.11}$$

This power law is the result of the special form (2.3) of the ledge interaction, whereas (2.7) is completely general. If, for instance, the ledge interaction were repulsive on short distances but had an attractive tail, then $f'(l)$ would be negative only up to a largest terrace width $l_{\max}$. Then (2.7) would imply that the rounded part of the crystal surface meets the facet at a finite angle, i.e., there would be a discontinuity in the slope $\Delta z'=l_{\max}^{-1}$.

Three important properties of (2.11) will be modified by the fluctuations to be discussed in the subsequent sections. The first is the scaling of the shape with the inverse of the supersaturation. The corrections to the shape scale differently, so that their relative size vanishes in the limit $c\to 0$. The second property of (2.11) is that the curvature of the surface diverges close to the facet rim:

$$z''(x)=(-c/2\pi)[c(x-R)]^{-1/2} \ . \tag{2.12}$$

This singularity will be smeared out due to the finite size of the bar. Finally, for $0<x<R$ the surface will no longer be perfectly horizontal as in (2.11): Fluctuations of the facet rim lead to an average cross section of the bar with $z'(x)\neq 0$ everywhere (apart from $x=0$).

In addition to these properties close to the facet, it will be useful to recall how the global dimensions of the cross section, $R$, $p$, and $L$, are determined by $\lambda$. First, we notice that (2.7) implies

$$p=-f'(l_p)/\lambda \ . \tag{2.13}$$

On the other hand, inserting (2.1) into (1.15) leads to the condition

$$f'(l_p)+\alpha=\lambda L \ ,$$

which combined with (2.13) yields

$$p+L=\alpha/\lambda \ . \tag{2.14}$$

Minimizing the free energy with respect to $p$, (1.16), gives the equilibrium values of $R$. If $p$ is increased by 1 keeping $L$ and all $l_m$ fixed, then necessarily $R$ decreases by $l_p$:

$$R\to R-l_p, \quad x_m\to x_m-l_p \ . \tag{2.15}$$

The corresponding change of the free energy,

$$\delta\Omega=f(l_p)+\lambda p l_p-\lambda L+\tau \ ,$$

should vanish; thus

$$L=\tau/\lambda+pl_p+f(l_p)/\lambda \ . \tag{2.16}$$

Now we show that the last two terms on the right-hand side can be identified with $L-R$ so that (2.16) leads to the well-known result

$$R=\tau/\lambda \ , \tag{2.17}$$

i.e., the facet size is proportional to the ledge free energy per unit length.[2] Treating $m$ as a continuous variable one can rewrite (2.7) in the form

$$df/dm=-\lambda m\, dl/dm=-\lambda\, d(ml-x)/dm \ .$$

In the last step (2.8) has been used. Integration yields

$$f(l_m)/\lambda=x_m-R-ml_m \ ;$$

hence for $m=p$

$$pl_p+f(l_p)/\lambda=L-R-l_p \ .$$

Since $l_p$ can be neglected compared to $L-R$ in the limit of small $\lambda$, this completes the derivation of (2.17).

Equations (2.13)–(2.17) show that all characteristic lengths $L$, $R$, and $p$ are inversely proportional to the supersaturation $\lambda$.

Now we come back to the question of what can be learned about the function $f(l)$ if one knows that the equilibrium shape has no edge at $x=L$, i.e., that $l_p=1$. Eliminating $L$ from (2.14), (2.16), and inserting (2.13), one finds that $f$ must obey the equation

$$f(1)-2f'(1)=\alpha-\tau \ . \tag{2.18}$$

## III. TRANSFER-MATRIX METHOD

The transfer-matrix method used by Villain[13] will now be extended to the case described in Sec. I. Our aim will be to evaluate the partition function

$$Z(p,L)=\mathrm{Tr}\exp(-\beta\mathcal{H})=\mathrm{Tr}\Theta^N \tag{3.1}$$

with $\mathcal{H}$ given by (1.20). The trace is to be performed over all ledge configurations $x_i(y)$, $i=1,\ldots,p$, or all eigenstates of the transfer matrix $\Theta$. As usual it suffices to determine the largest eigenvalue of the transfer matrix if the rod is very long. It can be obtained easily if the potential $v$ in (1.6) is assumed to have the form

$$v(x)=\begin{cases}\infty & (x\le 0)\\ 0 & (x>0) \ .\end{cases} \tag{3.2}$$

Consider the matrix element $\langle\phi|\Theta|\psi\rangle$, where

$$|\psi\rangle=|x_1,x_2,\ldots,x_p\rangle \tag{3.3}$$

is a possible ledge configuration at constant $y$ and, similarly, $|\phi\rangle$ represents the state of the cross section at $y+1$. If $|\psi\rangle=|\phi\rangle$ it is simply given by [cf. (1.4)]

$$\langle\phi|\Theta|\psi\rangle=\exp\left[\beta\lambda\sum_m x_m\right] \quad \text{if } |\psi\rangle=|\phi\rangle \ . \tag{3.4}$$

If $|\psi\rangle$ and $|\phi\rangle$ differ by just one kink in the $q$th ledge, then the matrix element is

$$\langle\phi|\Theta|\psi\rangle=\exp\left[-\beta\tau_1+\beta\lambda\sum_m x_m\right] \quad \text{if } \langle\phi|x_m|\phi\rangle-\langle\psi|x_m|\psi\rangle=\pm\delta_{mq} \ . \tag{3.5}$$

It is convenient to consider only low temperatures, $\beta\tau_1\gg 1$, where matrix elements between successive states

that differ by more than one kink can be neglected. Then (3.4) and (3.5) are all we need to characterize the transfer matrix.

Let $|\phi\rangle$ and $|\psi\rangle$ satisfy

$$x_{m-1}<x_m<x_{m+1}\ . \tag{3.6}$$

Then (3.3) can be written in terms of fermion operators as

$$|\psi\rangle=c_{x_1}^{\dagger}c_{x_2}^{\dagger}\cdots c_{x_p}^{\dagger}|0\rangle\ ,$$

where $c_x^{\dagger}$ creates a fermion at $x$, and $|0\rangle$ is the state with no fermion. Equations (3.4) and (3.5) can now be combined into a single expression:

$$\langle\phi|\Theta|\psi\rangle=\langle\phi|\Theta_1|\psi\rangle\langle\psi|\Theta_2|\psi\rangle$$

with

$$\Theta_1=1+e^{-\beta\tau_1}\sum_x(c_x^{\dagger}c_{x+1}+\text{ H.c.})$$

$$\approx\exp\left[e^{-\beta\tau_1}\sum_x(c_x^{\dagger}c_{x+1}+\text{ H.c.})\right] \tag{3.7}$$

and

$$\Theta_2=\exp\left[\beta\lambda\sum_x xc_x^{\dagger}c_x\right]\ . \tag{3.8}$$

In (3.7) we used the abbreviation H.c. to denote the Hermitian-conjugate operator. On easily checks that the matrix element of $\sum_x(c_x^{\dagger}c_{x+1}+\text{H.c.})$ is 1 between states that differ by exactly one kink, and 0 otherwise.

One can simplify the problem further in the limit where

$$\beta\lambda\ll 1\ll\beta\tau_1\ . \tag{3.9}$$

Then one can apply the Baker-Hausdorff formula

$$\exp A\,\exp B=\exp(A+B+\tfrac{1}{2}[A,B]$$

$$+\text{higher-order commutators})\ ,$$

and neglect all commutators in the exponent. Therefore, the transfer matrix may be written as the exponential of a simple operator:

$$\Theta=\exp(-\beta H)\ , \tag{3.10}$$

with

$$H=-\sum_x[G(c_x^{\dagger}c_{x+1}+\text{ H.c.})+\lambda xc_x^{\dagger}c_x]\ , \tag{3.11}$$

where $G$ is given by (2.5).

If one knows the ground-state energy $E_0$ of $H$ one can immediately calculate the partition function (3.1) and from that the free energy in the limit of large $N$:

$$\Omega=(\alpha L+\tau_0 p-\lambda L^2/2+E_0)N\ . \tag{3.12}$$

Moreover, the ground state $|E_0\rangle$ of $H$ contains information about the profile of the rod (Fig. 1) averaged over thermal fluctuations. Since $\langle E_0|c_j^{\dagger}c_j|E_0\rangle$ is the probability of finding a ledge at position $x=j$, the average profile is given by

$$z(x)=-\sum_{j<x}\langle E_0|c_j^{\dagger}c_j|E_0\rangle\ . \tag{3.13}$$

With this definition the height $z(0)$ of the top of the surface is very close to zero.

Equation (3.11) is a Hamiltonian of noninteracting fermions in an external potential. The ground state for $p$ fermions is therefore

$$|E_0\rangle=\prod_{k=1}^{p}a_k^{\dagger}|0\rangle\ , \tag{3.14}$$

with energy

$$E_0=\sum_{k=1}^{p}\varepsilon_k\ . \tag{3.15}$$

$k$ labels the various one-fermion eigenstates, $a_k^{\dagger}$ creates a fermion in state $k$, an the $k$'s are ordered according to increasing eigenvalues $\varepsilon$ of (3.11), i.e.,

$$Ha_k^{\dagger}|0\rangle=\varepsilon_k a_k^{\dagger}|0\rangle,\quad \varepsilon_1\le\varepsilon_2\le\varepsilon_3\le\cdots\ . \tag{3.16}$$

The Fermi operators $a_k$ can be expressed in terms of the $c_x$'s:

$$a_k^{\dagger}=\sum_x\psi_k(x)c_x^{\dagger}\ . \tag{3.17}$$

The wave function $\psi_k(x)$ fulfills the equation

$$-G[\psi_k(x+1)+\psi_k(x-1)]-\lambda x\psi_k(x)=\varepsilon_k\psi_k(x)\ , \tag{3.18}$$

which is easily derived by inserting (3.17) and (3.11) into (3.16).

The easiest way to get a qualitative understanding of the solutions of this equation is to take the continuum limit of the discrete spacial lattice. We shall argue later that the results are meaningful also quantitatively. Introducing the dimensionless supersaturation $c$ and energy $\tilde{\varepsilon}$,

$$c=\lambda/G,\quad \tilde{\varepsilon}=\varepsilon/G+2\ , \tag{3.19}$$

and recognizing $\psi(x+1)-2\psi(x)+\psi(x-1)$ as the lattice version of $d^2\psi/dx^2=\psi''(x)$, the continuum version of (3.18) reads

$$-\psi_k''(x)-cx\psi_k(x)=\tilde{\varepsilon}_k\psi(x)\ . \tag{3.20}$$

This is the Schrödinger equation for an electron in an electric field, a standard example in quantum-mechanics textbooks (see, e.g., Ref. 14).

However, the boundary conditions in this case are not the usual ones. None of the fermions can go beyond $x=L$, which corresponds to an impenetrable wall at $x=L$ (Fig. 3); hence

$$\psi(L)=0\ . \tag{3.21}$$

The boundary condition at the left is trickier, since we have completely ignored so far the possibility that the facet might form islands, or in the fermion language, that a fermion (downward ledge) annihilates with an antifermion (upward ledge) from the interval $(-L,0)$. In Sec. V this will be justified by showing that the rate of island formation on macroscopic facets is so small that its

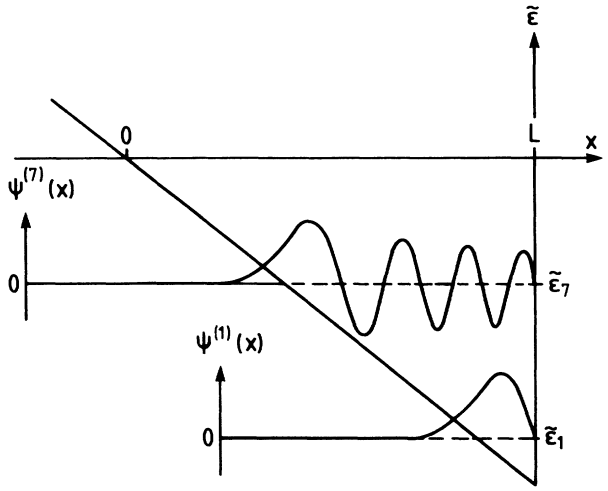


FIG. 3. Schematic eigenfunctions of an electron in an electric field with a wall at $x=L$: ground state $\psi^{(1)}$ and sixth excited state $\psi^{(7)}$ (up to normalization factors).

influence on the ledge fluctuations can be neglected. This means that we may regard the facet to extend to $x=-\infty$ (Fig. 3), as far as the configurations of the ledges are concerned. Then only the solutions vanishing for $x\to-\infty$ need to be considered,

$$\psi(x\to-\infty)=0 \ . \tag{3.22}$$

The other ones, increasing exponentially, are not normalizable.

It is immediately clear that the characteristic length scale in (3.20) is $c^{-1/3}$ while the energy $\tilde{\varepsilon}$ should be measured in units of $c^{2/3}$. Introducing the scaled quantities

$$\xi=c^{1/3}x+e, \quad e=c^{-2/3}\tilde{\varepsilon} \tag{3.23}$$

removes the parameters $c$ and $\tilde{\varepsilon}$ from the Schrödinger equation (3.20):

$$\left[\frac{d^2}{d\xi^2}+\xi\right]\varphi(\xi)=0 \ , \tag{3.24}$$

where

$$\psi(x)=A\varphi(\xi)=A\varphi(c^{1/3}(x+\tilde{\varepsilon}/c)) \tag{3.25}$$

with an appropriate normalization factor $A$. In the limit of small supersaturation $c$, $\psi(x)$ is a slowly varying function of $x$. This justifies the continuum approximation (3.20).

It is well known[4] that the solution of (3.24) satisfying the boundary condition (3.22) is the Airy function,

$$\varphi(\xi)=\frac{1}{\sqrt{\pi}}\int_0^\infty du\,\cos\left[\frac{u^3}{3}-\xi u\right] . \tag{3.26}$$

Its asymptotic behavior is oscillatory for $\xi\to\infty$,

$$\varphi(\xi)\approx\xi^{-1/4}\sin(\tfrac{2}{3}\xi^{3/2}+\pi/4) \ , \tag{3.27}$$

and exponentially decaying for $\xi\to-\infty$,

$$\varphi(\xi)\approx\tfrac{1}{2}|\xi|^{-1/4}\exp(-\tfrac{2}{3}|\xi|^{3/2}) \ . \tag{3.28}$$

According to (3.21) the corresponding wave function $\psi$ has to vanish at $x=L$, i.e.,

$$\varphi(c^{-2/3}(cL+\tilde{\varepsilon}))=0 \ . \tag{3.29}$$

The zeros of the Airy function thus determine the energy spectrum (see Fig. 3). Let $\xi_1<\xi_2<\xi_3<\cdots$ be the zeros of $\varphi(\xi)$. Then the $k$th energy level is given by

$$\tilde{\varepsilon}_k=-Lc+c^{2/3}\xi_k \ . \tag{3.30}$$

The asymptotic behavior (3.27) gives the following expression for $\xi_k$:

$$\xi_k=\left[\frac{3\pi}{2}(k-\tfrac{1}{4})\right]^{2/3} \tag{3.31}$$

which is an excellent approximation not only for large $k$ but even down to $k=1$. The first zero, $\xi_1$, agrees with (3.31) within 1%.[15]

It remains to determine the normalization $A_k$ of the corresponding eigenfunction $\psi_k(x)$, (3.25). In Appendix A we show that for $k\gg1$

$$A_k\approx\left[\frac{3\pi}{2}\frac{k}{c}\right]^{-1/6} . \tag{3.32}$$

Equations (3.25) and (3.30)–(3.32) are the basic results of our calculation. Now we are in the position to discuss their physical implications for the free energy [(3.12) and (3.15)] per unit length of the bar,

$$\omega=\Omega/N=\alpha L+\tau_0 p-\lambda L^2/2+\sum_{k=1}^{p}\varepsilon_k \ . \tag{3.33}$$

It is minimal with respect to $p$ if all levels below the "Fermi energy" $(-\tau_0)$ are occupied:

$$\varepsilon_p\le-\tau_0\le\varepsilon_{p+1} \ . \tag{3.34}$$

With (2.4), (3.19), (3.30), and (3.31) this implies

$$\tau/\lambda\approx-\tilde{\varepsilon}_p/c\approx L-\frac{1}{c}\left[\frac{3\pi}{2}cp\right]^{2/3} . \tag{3.35}$$

According to (2.9) the second term on the right-hand side can be identified with $L-R$, so that (3.35) is equivalent to (2.17). Similarly, stationarity with respect to $L$, (1.15), implies, using (3.19) and (3.30),

$$\alpha=\lambda L-\sum_{k=1}^{p}\frac{\partial\varepsilon_k}{\partial L}=\lambda(L+p) \ , \tag{3.36}$$

in agreement with (2.14).

These results are, of course, not surprising. We take only thermal fluctuations of the ledges into account and do not investigate fluctuations in $L$ or in $p$ so that they obey the same relations as in Sec. II. This procedure is justified because we are mainly interested in the finite-size corrections to the profile (2.11) close to the facet. How it is modified by the fluctuations will be discussed in the next section.

## IV. SURFACE FLUCTUATIONS

The results derived in Sec. III contain information about the fluctuation properties of the facet edge. One can easily determine two characteristic lengths: A correlation length $\xi_\parallel$ parallel to the global ledge direction (i.e., the $y$ direction), and a transverse one, $\xi_\perp$, parallel to the $x$ direction.

The physical meaning of $\xi_\parallel$ can best be explained by considering the probability $p(x,y)$ that any ledge goes through the point $(x,y)$ given that there was a ledge at $(x,0)$. Asymptotically it decays like $\exp(-y/\xi_\parallel)$. Using the transfer-matrix technique one calculates

$$p(x,y)\sim\langle E_0|c_x^\dagger c_x|E_0\rangle+\exp(-y/\xi_\parallel)|\langle E_0|c_x^\dagger c_x|E_1\rangle|^2/\langle E_0|c_x^\dagger c_x|E_0\rangle\ , \tag{4.1}$$

where $\xi_\parallel$ is proportional to the inverse energy gap between the ground state and the first excited state $E_1$ of the fermion system. From (3.19), (3.30), and (3.31) one obtains

$$\xi_\parallel^{-1}=\beta(\varepsilon_{p+1}-\varepsilon_p)=\beta\pi\lambda\left[\frac{3\pi}{2}cp\right]^{-1/3}\propto\lambda\ . \tag{4.2}$$

$\xi_\parallel$ is the *largest* length scale over which correlations in the ledge position are sustained. It must not be confused with the typical distance of collisions between the facet rim and the second ledge.[16] This smaller length (which can be shown to be proportional to $c^{-2/3}$) should not depend on the total number $p$ of ledges, in contrast to (4.2). $\xi_\parallel$ describes correlations due to collective fluctuations of the ledge system as a whole. It is inversely proportional to the supersaturation $\lambda$, just as the macroscopic lengths $L$, $p$, and $R$. The asymptotic form (4.1) is only valid for $y\gg\xi_\parallel$. On smaller distances one has to take the other eigenvalues of the transfer matrix into account, too.

The second length we want to discuss is the typical amplitude $\xi_\perp$ of the wandering of the facet rim about its average position $R$. Due to these fluctuations the thermal average of the profile $z(x)$ is not a constant for $0<x<R$. But the deviation $\delta z(x)$ is small if $x\ll R-\xi_\perp$: It will now be shown that $\delta z(x)$ decays like

$$\exp\{-\tfrac{4}{3}[(R-x)/\xi_\perp]^{3/2}\}$$

inside the facet, and that

$$\xi_\perp=c^{-1/3}\ . \tag{4.3}$$

Inserting (3.14) and (3.17), the average slope of the surface is

$$z'(x)=-\langle E_0|c_x^\dagger c_x|E_0\rangle=-\sum_{k=1}^{p}|\psi_k(x)|^2\ . \tag{4.4}$$

In Appendix B it is shown that (4.4) becomes, upon insertion of (3.25)–(3.32),

$$z'(x)=-\frac{1}{\pi}\int_{c(x-L)}^{c(x-R)}d\omega|\omega|^{-1/2}\chi(c^{-2/3}\omega)\ , \tag{4.5}$$

up to terms which are small by a factor $c^{1/3}$. Here,

$$\chi(\xi)=|\xi|^{1/2}\varphi^2(\xi) \tag{4.6}$$

vanishes exponentially for $\xi\to-\infty$ and is the squared sine part of (3.27) for $\xi\to\infty$. The upper integration boundary contains the facet size $R$ in the absence of fluctuations, as defined by (2.17) and (3.35).

Now, if $x\ll R$, the argument of $\chi$ will always be negative, and hence $z'(x)$ will be exponentially small, but nonzero. Deep inside the facet, fluctuations modify the profile (2.11) only by a small amount, of the order of

$$\delta z(x)\approx\frac{c}{16\pi}[c(R-x)]^{-3/2}\exp\left[-\frac{4}{3c}[c(R-x)]^{3/2}\right] \tag{4.7}$$

(see Appendix C for the calculation). With (4.3) this is the above-mentioned result.

If the integration in (4.5) extends into the region where $c^{-2/3}\omega\geq-1$, significant deviations from (4.7) will occur because $\chi$ is no longer exponentially small. This condition is equivalent to

$$R-x\leq c^{-1/3}=\xi_\perp \tag{4.8}$$

and means that one has entered the interval over which the rim of the facet typically fluctuates.

It is important to notice that the Airy function and hence the integrand in (4.5) are bounded everywhere notwithstanding the singular factor $|\omega|^{-1/2}$ in (4.5). For $|\omega|\gg c\xi_\perp=c^{2/3}$ one may use the asymptotic expression (3.27) for the Airy function. For $x-R\gg\xi_\perp$ one can thus replace (4.5) by

$$z'(x)\approx-\frac{1}{\pi}\int_0^{c(x-R)}d\omega\,\omega^{-1/2}\sin^2\left[\frac{2}{3c}\omega^{3/2}+\frac{\pi}{4}\right]+O(c^{2/3})\ . \tag{4.9}$$

The sine squared oscillates so quickly for $c\to0$ that one may replace it by its average value $\frac{1}{2}$ in the integral; hence

$$z'(x)\approx-(1/\pi)[c(x-R)]^{1/2}\ . \tag{4.10}$$

In the limit $c\to0$ corresponding to an infinite diameter of the bar we thus reproduce the power-law behavior (2.11) implying a divergent curvature at the rim of the facet. Notice that this singularity is directly related to the singular factor $|\omega|^{-1/2}$ in (4.5), which is actually compensated by the function $\chi$ if one takes fluctuations into account properly.

The actual curvature of the surface close to $x=R$ is obtained from (4.5):

$$z''(x)=-(c/\pi)|c(x-R)|^{-1/2}\chi(c^{1/3}(x-R))$$
$$=-(1/\pi)c^{2/3}\varphi^2(c^{1/3}(x-R)) , \quad (4.11)$$

where the Airy function $\varphi$ is perfectly smooth at $x=R$. [The contribution from the lower integration boundary is exponentially small and has been neglected in (4.11).] This shows that the singularity (2.12) is smeared out on the scale $c^{-1/3}=\xi_\perp$, as expected.

## V. ISLAND FORMATION AND DECAY OF A BAR

As already mentioned, the calculations of the preceding sections ignored the possibility of island formation on the upper facet. Fluctuations like these will ultimately lead to a decay of the translationally invariant bar shape, which, of course, is not the true equilibrium shape of the material. However, this decay will be seen to be very slow for large diameters.[17] It is an activated process, the activation barrier being due to the ledge parts perpendicular to the $y$ direction required by any change of $L$ or $p$.

Any deviation of the number of ledges from its optimal value $p$, determined by (3.34), increases the free energy if $L$ is kept constant. Therefore, these fluctuations are not responsible for the decay of the bar. This is in contrast to fluctuations of $L$ for fixed $p$ (Fig. 4) that lead to an instability of the bar.

Suppose the value of $L$ is constant along the bar apart from an interval of length $Y$ where it deviates by $\Delta L=\pm 1$. This costs a free energy

$$\Delta\Omega=Y\Delta\omega+Ls\tau . \quad (5.1)$$

The second term is due to the ledge parts perpendicular to the bar direction in the region where $L$ changes, and $s$ is a positive coefficient of order unity depending, e.g., on the island shape. The free-energy difference per unit length, $\Delta\omega$, is obtained from (3.30) and (3.33):

$$\Delta\omega=[\alpha-\lambda(L+p)]\Delta L-\lambda(\Delta L)^2/2 .$$

If the values of $L$, $p$, and $\lambda$ are adjusted according to (3.36), the first term vanishes, so that

$$\Delta\omega=-\lambda/2 . \quad (5.2)$$

Therefore, (5.1) becomes negative for

$$Y>L\lambda^{-1}2s\tau\propto L^2 , \quad (5.3)$$

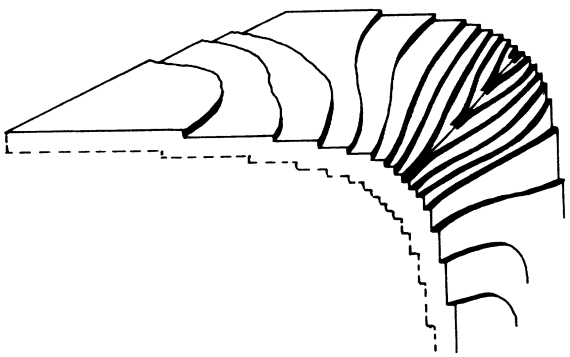

FIG. 4. Fluctuation of the bar diameter.

which means that the bar is unstable for long-wavelength fluctuations in $L$. As the sign of $\Delta L$ does not matter, one can always arrange bulges ($\Delta L>0$) and constrictions ($\Delta L<0$) in such a way that the volume of the bar, $V_c$, remains constant. Then the quadratic term in (1.10) is zero and hence cannot stabilize the bar against these fluctuations.

What is the characteristic time until such a bulge nucleates on a bar which was prepared ideally with $L$ and $p$ constant? As long as a bulge does not go all around the bar but covers only a finite portion $q<1$ of the circumference, (5.1) has to be replaced by

$$\Delta\Omega\approx q(-Y\lambda/2+Ls\tau)+Ys'\tau . \quad (5.4)$$

The last term is due to the boundaries of the bulge parallel to the bar direction, and $s'$ is a positive geometry factor of order unity. It vanishes if the bulge goes all around the bar (i.e., $q=1$). If the facet width $R=\tau/\lambda$ is much larger than 1, the positive last term in (5.4) dominates over the first one. Hence $Y$ remains small, as long as the bulge is not completed. The nucleation barrier is therefore $Ls\tau$, so that the characteristic time for the nucleation of a bulge (or constriction, by analogy) is, according to standard nucleation theory (e.g., Ref. 18),

$$t_{\rm nucl}\approx\exp(\beta Ls\tau) . \quad (5.5)$$

For small temperatures and large samples it takes an extremely long time for a perfectly cut bar to begin to decay into crystallites. Thus the assumptions made in the derivation of the ledge fluctuations in the preceding sections are justified.

## VI. CONCLUSION

In order to summarize our main results, we distinguish two categories of lengths which are important for the shape of a cylindrical crystal bar with facets. The first type scales with the inverse supersaturation $\lambda^{-1}$. It is well known that the diameters of the bar and the facets belong into this category. In this paper we have shown that the length $\xi_\parallel$, (4.2), over which the ledge positions remain correlated is proportional to these characteristic dimensions of the cross section of the bar.

The second type scales only with $\lambda^{-1/3}$. These lengths are vanishingly small compared to those in the first category if the size of the bar becomes large (i.e., $\lambda\to 0$). A well-known example is the width $l_m$, (2.8), of the $m$th terrace which increases only as $\lambda^{-1/3}$ [see (2.9)]. This is the reason why the terraces are qualitatively different from the facet, and look like a continuously rounded surface in experiments on large samples. We have shown that the amplitude $\xi_\perp$ of the fluctuation of the facet rim is of the same order of magnitude as the width of the first terrace. This implies that even in the vicinal regime ledges are not well separated: Their average positions are not much further apart than the distances over which they typically wander. Notice, however, that we have only taken the steric repulsion between ledges into account. The elastic repulsion[19] might alter this conclusion. The singularity found in the curvature close to the facet if fluctuations are neglected as in the Wulff con-

struction is actually smeared out over the interval $\xi_\perp$. The power law (2.11) can only be observed in a distance from the facet rim which is much larger than $\xi_\perp$.

There is an interesting relation between our results and complete wetting in two dimensions. In this case, one considers a single line instead of $p$ ledges. It represents the interface between a liquid layer attracted to the substrate at $x=L$ and the vapor phase. As long as $c>0$ the (two-dimensional) bulk prefers to be in the vapor phase so that the wetting layer has finite thickness $l_1 \sim \xi_\perp$ (see, e.g., Ref. 20). As one approaches phase coexistence ($c \to 0$) the wetting layer becomes thicker and thicker: $\xi_\perp$ diverges as $c^{-1/3}$. At the same time the correlation length parallel to the interface diverges as $c^{-2/3}$.[20] This may be regarded as a special case of our result (4.2) for $p=1$.

The lengths $\xi_\parallel$ and $\xi_\perp$ should not be confused with those introduced in Ref. 21, also in the context of equilibrium shapes of crystals. The difference becomes most obvious if one considers a tilted, flat surface, i.e., $\lambda$ is zero but the density of ledges, $p/L$, is finite. Then the correlation functions decay algebraically,[22] in agreement with our result that the correlation lengths $\xi_\parallel$ and $\xi_\perp$ are infinite. In Ref. 21 $\xi_\parallel$ and $\xi_\perp$ have a different meaning: They describe the (finite) scales on which the algebraic decay occurs. For instance, $\xi_\perp$ has the meaning of the average distance between the ledges.

The key point of the calculation was to identify the ledges with free fermions in a triangular potential well. For simplicity we only considered the case of temperatures small compared to the kink energy, $k_B T \ll \tau_1$, so that we could neglect kink interactions. We concentrated on the leading corrections to the Wulff shape by requiring that $\lambda \ll k_B T$. This allowed us to use the Hamiltonian limit (3.10) of the transfer matrix and to solve the fermion system in the continuum limit.

The most basic assumption we made is that the bar geometry is reasonably stable to permit the development of a (quasi)equilibrium of the ledge fluctuations already described. Therefore, we estimated the characteristic nucleation time (5.5) for bulges and constrictions along the bar—typical fluctuations which trigger its decay into crystallites. For small supersaturation this time turns out to be exponentially large (provided, of course, that $\tau$ and $\alpha$ are not too small compared to $k_B T$, so that macroscopic dimensions $R$ and $L$ are guaranteed). Therefore our assumption is justified if the bar has been prepared carefully enough, i.e., without many bulges and constrictions to begin with. In practice this will be difficult to achieve, so our theory needs future refinement in this direction in order to permit a comparison with experiments.

There is another constraint—a lower bound on the supersaturation—which has to be taken into account. It comes from the influence of gravitation on the equilibrium shape and has been pointed out recently by Avron and Zia.[10] Let us assume the $z$ axis is vertical (Fig. 1). In the presence of gravity the chemical potential and hence the supersaturation, too, depend linearly on the height:

$$\lambda(z)=\lambda(0)-gz \ , \tag{6.1}$$

where $\lambda(0)$ is the value just above the facet, $z=0$, and $g$ is the gravitational acceleration times $(\rho_c-\rho_{f0})$ [cf. (1.14)]. Accordingly (2.6) becomes

$$f'(\bar{x}_{m+1}-\bar{x}_m)=f'(\bar{x}_m-\bar{x}_{m-1})-\lambda(-m) \ ,$$

which implies, instead of (2.7),

$$f'(l_m)=-\sum_{n=1}^{m}\lambda(-n)=-\lambda(0)m-gm(m+1)/2 \ . \tag{6.2}$$

Consequently, the determination (2.9) of the profile is more complicated:

$$\bar{x}_{m+1}-R=\sum_{n=1}^{m}\left[\frac{3}{2\pi^2}[\lambda(0)n+gn(n+1)/2]\frac{1}{G}\right]^{-1/3} . \tag{6.3}$$

If $m \ll \lambda(0)/g$, the $\lambda(0)$ term in small parentheses dominates and leads to the power laws (2.9) and (2.11). However, if $m \gg \lambda(0)/g$, the $g$ term determines the behavior of (6.3). Then one obtains

$$\bar{x}_{m+1}-R \approx (6\pi)^{2/3}\left[\frac{G}{g}m\right]^{1/3} ,$$

or equivalently

$$z \approx -\frac{g}{G}\frac{1}{(6\pi)^2}(x-R)^3 \ . \tag{6.4}$$

In agreement with Ref. 10 we find an exponent 3 instead of $\frac{3}{2}$ which was found without gravitation.

We have shown that the power law (2.11) can only be observed for

$$x-R \gg \xi_\perp=[G/\lambda(0)]^{1/3} \ ,$$

i.e., in a vertical distance from the facet

$$|z| \gg 1 \ . \tag{6.5}$$

On the other hand, taking gravitation into account, $|z|=m$ must be much smaller than $\lambda(0)/g$. Otherwise one will see the crossover to the different power law (6.4). In order for the window to be large, where (2.11) can be observed, it is required that

$$g \ll \lambda(0) \ . \tag{6.6}$$

If would be nice if one could study the fluctuations of the shape in full generality, including the influence of gravity. However, it can be seen easily that this becomes a formidable task: In the fermion language gravity introduces a complicated interaction among the particles so that the Hamiltonian can no longer be straightforwardly diagonalized.

If the bar is not infinitely long but of a length comparable to $\xi_\parallel$, then it does not suffice to take into account the two largest eigenvalues of the transfer matrix only. This gives rise to additional finite-size corrections[23] to the equilibrium shape, e.g., to (4.1) and (4.4). This type of correction will be important if one wants to make a realistic comparison with experiments on more "cube-shaped" crystallites.

## ACKNOWLEDGMENTS

We would like to thank H. van Beijeren, who stimulated this research with several useful remarks. Discussions with R. Lipowsky and D. Kroll have been much appreciated.


## APPENDIX A

The normalization condition

$$\int_{-\infty}^{L} |\psi_k(x)|^2 dx = 1 \tag{A1}$$

is equivalent, according to (3.25), to

$$c^{1/3} A_k^{-2} = \int_{-\infty}^{\xi_k} \varphi^2(\xi) d\xi \ , \tag{A2}$$

where $\xi_k$ is the $k$th zero of the Airy function $\varphi$. for large $k$ one can use (3.27) to write

$$c^{1/3}( A_{k+1}^{-2} - A_k^{-2}) \approx \int_{\zeta_k}^{\zeta_{k+1}} (\tfrac{3}{2}\zeta)^{-2/3} \sin^2\zeta \, d\zeta \ , \tag{A3}$$

where $\zeta_k = \pi k$. It follows that

$$c^{1/3} \frac{dA_k^{-2}}{dk} = \left[ \frac{3\pi}{2} k \right]^{-2/3} \frac{\pi}{2} \left[ 1 + O\left[ \frac{1}{k} \right] \right] \ , \tag{A4}$$

which can be integrated to give (3.32).

## APPENDIX B

According to (4.4), (3.25), (3.30), and (3.31), the average slope of the surface is given by

$$z'(x) = -\sum_{k=1}^{p} A_k^2 \varphi^2(c^{-2/3}\omega(x,k)) \ , \tag{B1}$$

where

$$\omega(x,k) = c(x-L) + \left[ \frac{3\pi}{2} c(k - \tfrac{1}{4}) \right]^{2/3} . \tag{B2}$$

With $\kappa = ck$ one may replace the $k$ summation in (B1) by an integral in the limit of small $c$:

$$\sum_{k=1}^{p} \cdots = \frac{1}{c} \int_0^{pc} d\kappa \cdots \ , \tag{B3}$$

where $pc$ is a constant independent of $c$. Substituting $\omega$ as the integration variable gives

$$z'(x) = -\frac{1}{c\pi} \int_{\omega_0}^{\omega_1} d\omega \, A_{\kappa/c}^2 \left[ \frac{3\pi}{3} \left[ \kappa - \frac{c}{4} \right] \right]^{1/3} \times \varphi^2(c^{-2/3}\omega) \ . \tag{B4}$$

Up to corrections small by a factor $c^{2/3}$ (at most) the integration may be extended from

$$\omega_0 = c(x-L) \tag{B5}$$

through

$$\omega_1 = c(x-L) + \left[ \frac{3\pi}{2} cp \right]^{2/3} = c(x-R) \ , \tag{B6}$$

where we used (2.17) and (3.35) to identify $R$. From (3.32) we know that for $\kappa \gg c$

$$A_{\kappa/c}^2 \approx \left[ \frac{3\pi}{2} \frac{\kappa}{c^2} \right]^{-1/3} . \tag{B7}$$

The main error in this formula occurs when one neglects the integration constant in the integration of (A4). This error is small by a factor $c^{1/3}$. Inserting (B7) into (B4) one obtains up to corrections small by a factor $c^{1/3}$

$$z'(x) = -c^{-1/3} \frac{1}{\pi} \int_{\omega_0}^{\omega_1} d\omega \, \varphi^2(c^{-2/3}\omega) \ . \tag{B8}$$

With (4.6) this completes the derivation of (4.5).

## APPENDIX C

For $x \ll R$ one may use the asymptotic expression (3.28) in (4.6) and (4.5) so that

$$|z'(x)| \approx \frac{1}{4\pi} \int_{\omega_1}^{|\omega_0|} d\omega \, \omega^{-1/2} \exp\left[ -\frac{4}{3c} \omega^{3/2} \right] \tag{C1}$$

with $\omega_0, \omega_1$ given in (B5) and (B6). To get a rough estimate we extend the integration up to infinity. A substitution

$$\zeta = \tfrac{2}{3}\omega^{3/2} \tag{C2}$$

leads to

$$|z'(x)| \approx \frac{1}{4\pi} \int_{\zeta_1}^{\infty} d\zeta \frac{1}{\omega(\zeta)} \exp\left[ -\frac{2}{c}\zeta \right] . \tag{C3}$$

Replacing $\omega^{-1}$ by its maximal value one obtains an upper bound for the integral:

$$|z'(x)| \approx \frac{c}{8\pi} |\omega_1|^{-1} \exp\left[ -\frac{4}{3c} |\omega_1|^{3/2} \right] . \tag{C4}$$

The deviation $\delta z(x)$ from $z = 0$ deep inside the facet can now be estimated by

$$\delta z(x) \approx \int_0^x |z'(x')dx'| = \frac{1}{8\pi} \int_{\omega_1(x)}^{\omega_1(0)} d\omega_1 |\omega_1|^{-1} \exp\left[ \frac{-4}{3c} |\omega_1|^{3/2} \right] . \tag{C5}$$

Going through the same steps as above, one arrives at (4.7).

---

*Present address: DRF/GMDN, CENG, 85X, F-38041 Grenoble CEDEX, France.


[1] M. Wortis, in *Chemistry and Physics of Solid Surfaces,* edited by R. Vanselow (Springer, Berlin, 1988), Vol. VII.

[2] H. van Beijeren and I. Nolden, in *Structure and Dynamics of Surfaces II,* edited by W. Schommers and P. von Blanckenhagen (Springer, Berlin, 1987), p. 259.

[3] H. W. J. Blöte and H. J. Hilhorst, J. Phys. A **15**, L631 (1982); C. Jayaprakash, W. F. Saam, and S. Teitel, Phys. Rev. Lett. **50**, 2017 (1983); C. Jayaprakash, C. Rottman, and W. F.

Saam, Phys. Rev. B **30**, 6549 (1984); C. Rottman and M. Wortis, *ibid.* **29**, 328 (1984).
[4]J. J. Métois and J. C. Heyraud, Surf. Sci. **180**, 647 (1987).
[5]J. J. Saenz and N. Garcia, Surf. Sci. **155**, 24 (1985).
[6]H. J. Schulz, J. Phys. (Paris) **46**, 257 (1985).
[7]K. Binder and M. H. Kalos, J. Stat. Phys. **22**, 363 (1980).
[8]M. Uwaha and P. Nozières, in *Proceedings of the 1985 Oji International Seminar on Morphology and Growth Unit of Crystals* (Terra Scientific, Tokyo, to be published); D. E. Wolf and P. Nozières, Z. Phys. B **70**, 507 (1988).
[9]A. Ya. Parshin, J. J. Saenz, and N. Garcia, J. Phys. C **21**, L305 (1988).
[10]J. E. Avron and R. K. P. Zia, Phys. Rev. B **37**, 6611 (1988).
[11]E. E. Gruber and W. W. Mullins, J. Phys. Chem. Solids **28**, 875 (1967).
[12]V. L. Pokrovskii and A. L. Talapov, Phys. Rev. Lett. **42**, 65 (1979).
[13]J. Villain, in *Ordering in Strongly Fluctuating Condensed Matter Systems,* edited by T. Riste (Plenum, New York, 1980), p. 221.
[14]L. D. Landau and E. M. Lifshitz, *Quantum Mechanics,* Vol. 3 of *Course of Theoretical Physics* (Pergamon, London, 1958), Vol. 3, pp. 70 and 491.
[15]*Handbook of Mathematical Functions,* edited by M. Abramowitz and I. A. Stegun (Dover, New York, 1965), p. 446.
[16]A similar distinction can be made if one describes two interacting interfaces in an external field; see R. Lipowsky, Habilitation thesis, University of Munich, 1987.
[17]J. W. Cahn, Scr. Metall. **13**, 1069 (1979).
[18]J. D. Gunton, M. San Miguel, and P. S. Sahni, in *Phase Transitions and Critical Phenomena,* edited by C. Domb and J. L. Lebowitz (Academic, New York, 1983), Vol. 8, p. 267.
[19]V. I. Marchenko and A. Ya. Parshin, Zh. Eksp. Teor. Fiz. **79**, 257 (1980) [Sov. Phys.—JETP **52**, 129 (1980)].
[20]S. Dietrich, in *Phase Transitions and Critical Phenomena,* edited by C. Domb and J. L. Lebowitz (Academic, New York, 1988), Vol. 12, p. 1.
[21]C. Jayaprakash and W. F. Saam, Phys. Rev. B **30**, 3916 (1984).
[22]H. J. Schulz, Phys. Rev. B **22**, 5274 (1980).
[23]They have been studied by D. Kroll for flat surfaces.